

Available online at www.sciencedirect.com



Trans. Nonferrous Met. Soc. China 21(2011) 121-126

Transactions of Nonferrous Metals Society of China

www.tnmsc.cn

Microstructural evolution of melt-spun Mg-10Ni-2Mm hydrogen storage alloy

WU Ying^{1,2,3}, XING Na^{1,4}, LU Zhi-chao¹, HAN Wei¹, ZHOU Shao-xiong¹, J. K. SOLBERG², V. A. YARTYS^{2,3}

- 1. Central Iron & Steel Research Institute Group, Advanced Technology & Materials Co., Ltd., Beijing 100081, China; 2. Department of Materials Technology, Norwegian University of Science and Technology,
 - NO-7491 Trondheim, Norway; 3. Institute for Energy Technology, P.O. Box 40, N-2027 Kjeller, Norway;
 - 4. School of Materials Science and Engineering, Inner Mongolia University of Technology, Hohhot 100051, China

Received 22 November 2009; accepted 23 Feburay 2010

Abstract: The microstructural evolution of a Mg-10Ni-2Mm (molar fraction, %) (Mm=Ce, La-rich mischmetal) hydrogen storage alloys applied with various solidification rates was studied. The results show that the grain size of melt-spun ribbon is remarkably reduced by increasing the solidification rate. The microcrystalline, nanocrystalline and amorphous microstructures are obtained by applying the surface velocities of the graphite wheel of 3.1, 10.5 and 20.9 m/s, respectively. By applying the surface velocity of the graphite wheel of 3.1 m/s, the melt-spun specimen obtains full crystalline with a considerable amount of coarse microcrystalline Mg and Mg₂Ni except for some Mm-rich particles. The amount of nanocrystalline phases significantly increases with increasing the surface velocity of the wheel to 10.5 m/s, and the microstructure is composed of a large amount of nanocrystalline phases of Mg and Mg₂Ni particles. A mixed microstructure containing amorphous and nanocrystalline phases is obtained at a surface velocity of the wheel of 20.9 m/s. The optimal microstructure with a considerable amount of nanocrystalline Mg and Mg₂Ni in an amorphous matrix is expected to have the maximum hydrogen absorption capacity and excellent hydrogenation kinetics.

Key words: hydrogen storage materials; Mg-based alloys; rapid-solidification; microstructure; transmission electron microscopy

1 Introduction

Mg-based alloys are the most attractive materials for hydrogen storage because of their low cost, high hydrogen storage capacity and rich natural resources. However, high hydrogen desorption temperature (300 °C) and relatively slow kinetics of H-absorption/desorption make them still far from being practically applicable. In order to improve the hydrogen storage applicability of the Mg-based alloys, several methods such as adding transition metals and rare-earth elements have been employed to enhance the reaction thermodynamics and H-adsorption kinetics. Rapid solidification (RS)[1–9] method is an effective process for improving the hydrogen storage ability by grain refinement to nano-size level and even amorphous microstructures.

Compared with the conventional crystalline Mg-based alloys, nanocrystalline alloys as well as alloys containing nanocrystalline and amorphous phases exhibit much faster kinetics of H-absorption/desorption and

lower temperature of hydriding/dehydriding. The large number of interfaces and grain boundaries available in the nanocrystalline materials provide easy pathways for hydrogen diffusion and promote the absorption of hydrogen[1]. Nanocrystalline Mg₂Ni-based alloys are known to exhibit higher H-absorption capacity of 3%-3.5% (mass fraction) and faster kinetics of hydriding/dehydriding than crystalline Mg₂Ni[1, 10]. HUANG et al[11] reported that the amorphous alloy showed the $Mg_{65}Cu_{25}Nd_{10}$ best hydrogenation rate and the maximum hydrogen capacity (3.2%, mass fraction) in comparison with those of partially and completely crystallized microstructural states. For the Mg-Ni-Mm alloy with a high Mg content, it is hard to control the chemical composition due to lower melting point of Mg, especially by the RS method. Thus, the stable microstructure is the key to obtain the excellent hydrogen storage property. In the present study, microcrystalline, nanocrystalline amorphous Mg-10Ni-2Mm hydrogen storage alloys were prepared by RS processing, and the microstructure evolution under various cooling rates in the melt-spun ribbons was studied and compared with the as-cast master alloy focusing on obtaining a stable microstructure for large hydrogen absorption capacity.

2 Experimental

The master ingot of ternary Mg-10Ni-2Mm alloy was prepared by induction melting a mixture of 99.7% pure Ce and La-rich mischmetal that also contained Pr, 99.98% pure Mg and 99.98% pure Ni. The melt-spun ribbons were obtained by a single roller melt-spinning technique (graphite quenching disc with a diameter of 200 mm) in an argon atmosphere of 20 kPa, and the details of which were described elsewhere[12–13]. Prior to the RS, the pre-alloying process was applied to obtaining the as-cast alloy with expected microstructure by controlling the processing parameters. The surface velocity of the wheel was adjusted in three steps from 3.1, 10.5 to 20.9 m/s. The microstructure of the specimens was examined by X-ray diffractometer (XRD), scanning electron microscope (SEM) and transmission electron microscope (TEM) equipped with an energy-dispersive X-ray spectrometer (EDS).

3 Results and discussion

3.1 Microstructural refinement of as-cast alloy

The as-cast master alloy has a typical dendritic microstructure. As shown in Fig.1(a), the microstructures consisted of mainly Mg₂Ni with a size of 2-80 µm and a minor mischmetal-rich Mg-containing phase in a matrix of Mg. The mischmetal-rich phases were determined to be Mg₁₂Ce and Mg₁₇Mm₂ (bright contrast in the micrograph). The melt-spun alloy shows a refined microstructure by the RS processing at a surface velocity of the graphite wheel of 3.1 m/s, as shown in Fig.1(b), and the grain size of Mg₂Ni particles with bright contrast in a matrix of Mg is greatly reduced. The phase constitutes can be explained from the Mg-Ni-La ternary phase diagram. Three phases, the pure Mg, the intermetallic phases Mg₂Ni and Mg₁₂La, are determined in the alloy. Therefore, the RS processing is effective for reducing the grain size of the Mg-Ni-Mm alloy.

3.2 Phase constitutes and morphologies of as-cast and melt-spun alloy

Fig.2 shows XRD spectra of the as-cast and melt-spun Mg-10Ni-2Mm alloys with different solidification rates. For the as-cast alloy, four phases, i.e. Mg, Mg₂Ni, Mg₁₇Mm₂ and Mg₁₂Ce phases, are identified in Fig.2(a). The two former phases, Mg and Mg₂Ni,

show stronger peak intensities than the two latter phases, Mg₁₇Mm₂ and Mg₁₂Ce, giving an indication of the relative amounts of the phases. The narrow width of the diffraction peaks evidences the coarse grains in the as-cast alloy.

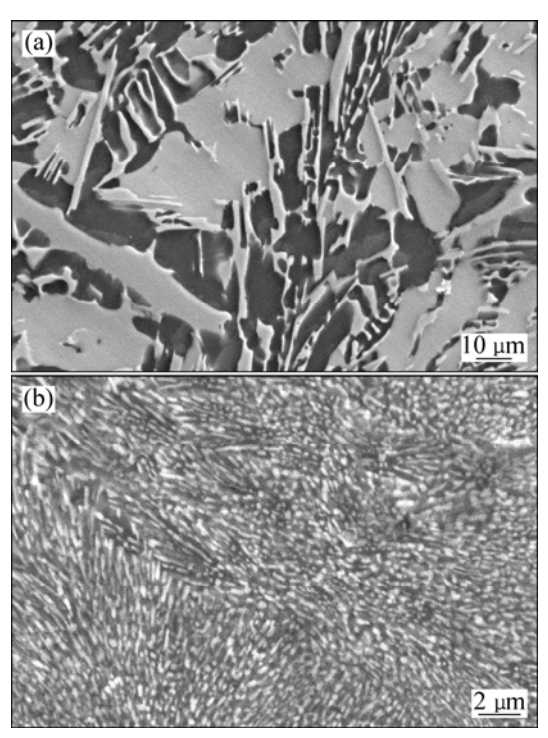


Fig.1 SEM images showing typical dendritic microstructure of as-cast Mg-10Ni-2Mm alloy consisting of mainly Mg₂Ni (gray areas) and minor mischmetal-rich Mg-containing phase (bright areas, Mg₁₂Mm and Mg₁₇Mm₂) in matrix of Mg (dark areas) (a), and refined microstructure of melt-spun alloy at surface velocity of graphite wheel of 3.1 m/s (b)

By applying the RS process, the microstructure of the hydrogen storage Mg-based alloy was refined. The phase constitutes in the microstructure varied with the solidification rate. Microcrystalline, nanocrystalline and amorphous microstructures in the Mg-10Ni-2Mm alloy were obtained at various solidification rates of the melt-spun ribbons. When the surface velocity of the graphite wheel was the lowest of 3.1 m/s, the lowest solidification rate was obtained, and the melt-spun specimen was fully crystalline. Three phases, i.e. Mg, Mg₂Ni and Mg₁₂Ce phases, are identified in Fig.2(b). The two former phases, Mg and Mg₂Ni, show stronger peak intensities than the latter phase, Mg₁₂Ce, showing much more amounts of the Mg and Mg₂Ni phases. Fig.3 shows TEM images of the melt-spun ribbon at the lowest solidification rate of 3.1 m/s. As shown in Fig.3(a), two types, i.e. rod-shaped and equiaxed grains, were observed. The precipitates that have rod-like morphology

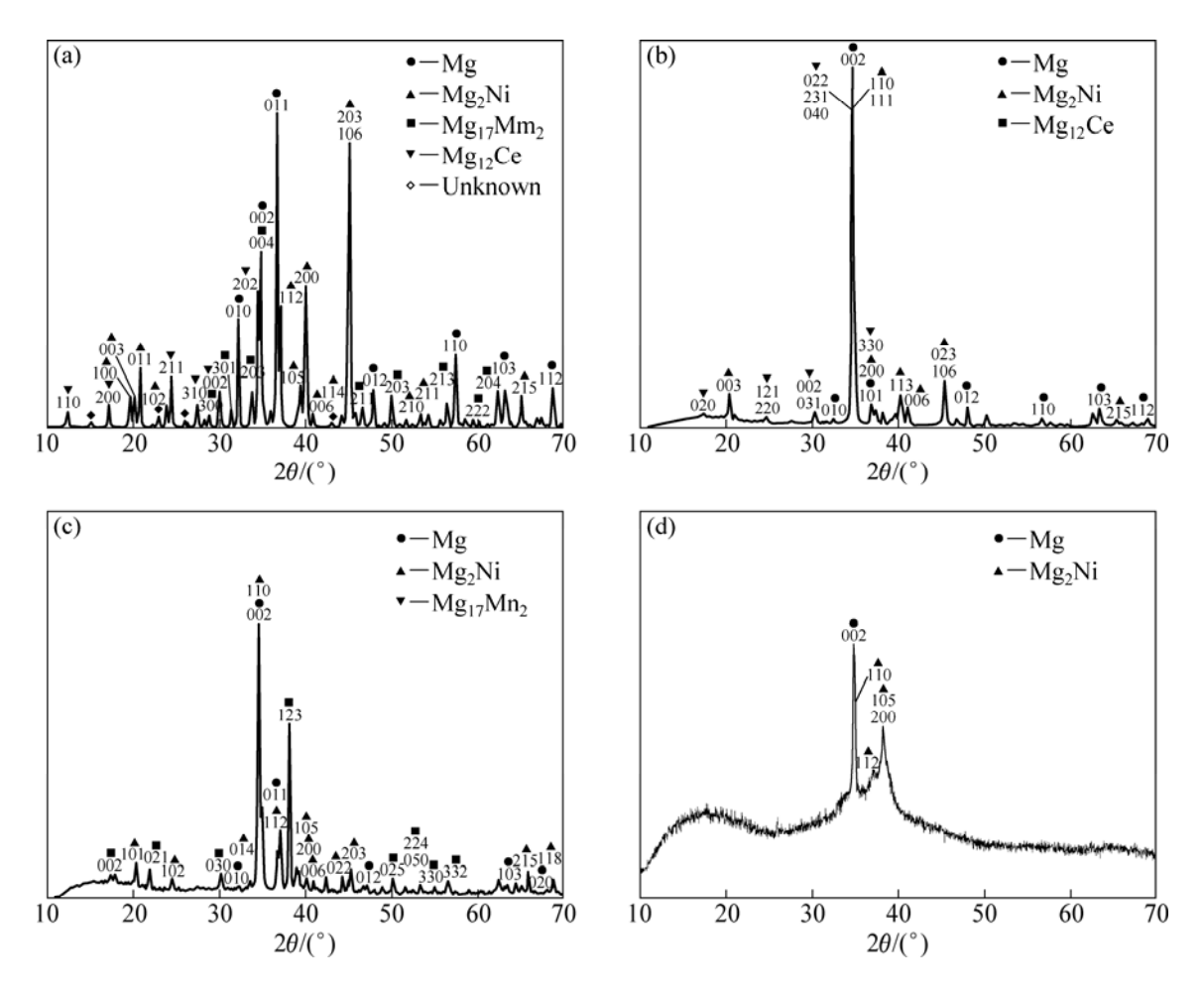
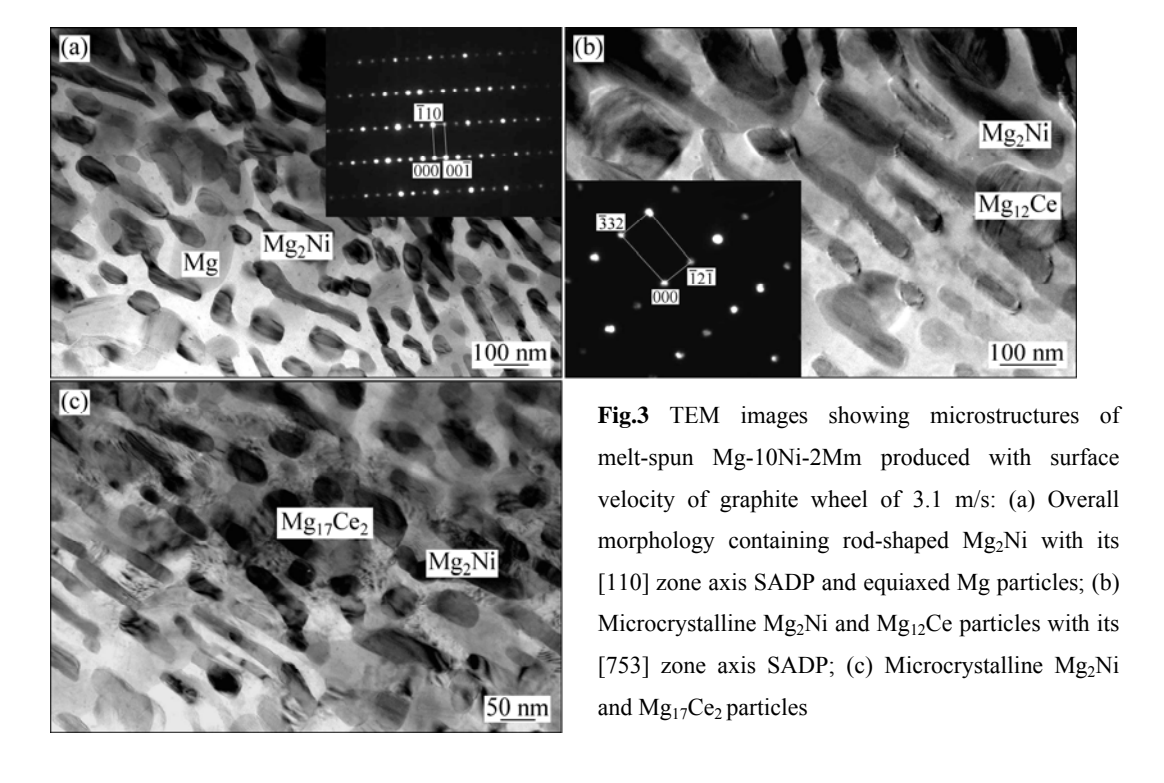


Fig.2 XRD spectra of as-cast alloy (a) and melt-spun Mg-10Ni-2Mm alloy solidified at different surface velocities of graphite wheel of 3.1 (b), 10.5 (c) and 20.9 m/s (d)



and average grain dimension of $0.8~\text{nm}\times~0.4~\mu\text{m}$ were identified as Mg_2Ni from electron diffraction [110] zone axis selected area diffraction pattern (SADP). The equiaxed grains were determined to be Mg particles with the average diameter of $0.2~\mu\text{m}$. From Fig.3(b), some equiaxed particles were determined to be mischmetal-rich $Mg_{12}Ce$ particle with a size of approximately $0.15~\mu\text{m}$ and its corresponding [753] zone axis SADP. Fig.3(c) shows a typical image containing $Mg_{17}Ce_2$ particles. Thus, the microstructure consists of mainly a considerable amount of microcrystalline Mg and Mg_2Ni and some $Mg_{12}Ce$ and $Mg_{17}Mm_2$ particles.

The nanocrystalline phases were obtained by increasing the surface velocity of the graphite wheel to 10.5 m/s. As shown in Fig.2(c), strong diffraction peaks of Mg and Mg₂Ni phases appeared in the specimen with this intermediate solidification rate. A small amount of Mg₁₇Mm₂ with weak peaks was also detected. Fig.4 shows typical TEM images of the microstructures of this melt-spun ribbon. In accordance with the result of XRD, a considerable amount of nanocrystalline grains were obtained in the specimen, as shown in Fig.4(a), showing nanocrystalline equiaxed Mg particles of about 80 nm size indicated by the inserted [243] zone axis SADP. It is obvious from Fig.4(b) that the Mg₁₇Ce₂ particles prefer

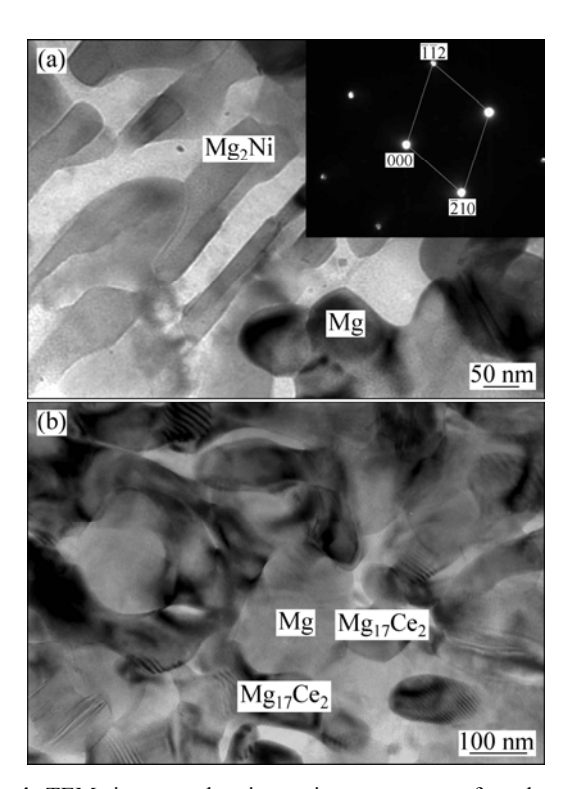


Fig.4 TEM images showing microstructures of melt-spun Mg-10Ni-2Mm with surface velocity of graphite wheel of 10.5 m/s: (a) Nanocrystalline mixtures of Mg particle with its [243] zone axis SADP and Mg₂Ni particles; (b) Nanocrystalline phases of Mg₁₇Ce₂ particles at boundary of Mg grain

to locate at the boundary of Mg grains. Thus, the microstructure is composed of a large amount of nanocrystalline phases of Mg and Mg₂Ni particles and a minor amount of mischmetal-rich phases.

By increasing the surface velocity of the graphite wheel to 20.9 m/s, the highest solidification rate of the melt-spun was obtained, resulting in the XRD spectrum with a lower intensity (Fig.2(d)) containing a broad maximum peak at $2\theta=12^{\circ}-25^{\circ}$ and some crystalline peaks for melt-spun ribbon. TEM image and its corresponding SADP are shown in Fig.5(a). Only featureless contrast over the entire bright field image and halo rings with no spotty diffraction patterns are clearly observable. However, some diffraction peaks from crystalline phases of Mg and Mg2Ni are occasionally observed, resulting in small peaks in the XRD spectrum. As shown in Fig.5(b), a considerable amount of nanocrystalline phases of Mg and Mg2Ni particles form in the amorphous matrix. Thus, the melt-spun ribbon is mainly composed of a mixture of amorphous single phase and a amount of nanocrystalline Mg and Mg2Ni particles.

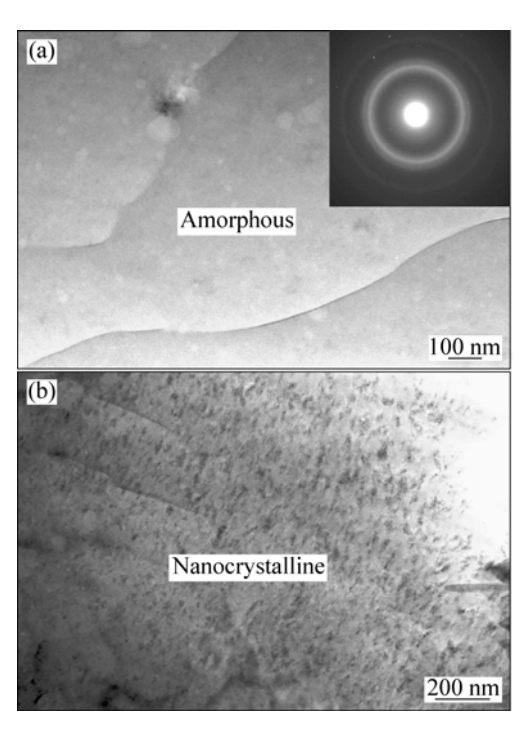


Fig.5 TEM images showing microstructures of melt-spun Mg-10Ni-2Mm alloy at surface velocity of graphite wheel of 20.9 m/s: (a) Amorphous matrix and its corresponding SADP; (b) Mixed nanocrystalline phases of Mg and Mg₂Ni particles

From above studies, various microstructures such as microcrystalline, nanocrystalline and amorphous phases are obtained by controlling the cooling rate of the melt-spun ribbon during the solidification. Compared with the as-cast master alloy in Fig.1(a), the grain size of

melt-spun ribbon is remarkably reduced by RS, and mico- and nano-size grains are obtained (see Figs.3-5). Previous work has demonstrated the improved hydrogen storage properties in Mg due to the large amounts of amorphous phases and fine nano-size particles. For a nanocrystalline Mg₆₃Ni₃₀Y₇ alloy[1], it was reported that the maximum hydrogen absorption capacity (about 3.0%, mass fraction) after melt spinning was found to exceed that of conventionally prepared polycrystalline Mg₂Ni. SPASSOV et al[10, 14] studied hydrogen storage of rapidly solidified Mg-based Mg-Ni-RE (RE=Y or Mm) alloys. They reported that the best hydriding properties were obtained in the nanocrystalline/amorphous Mg₇₅Ni₂₀Mm₅ alloy with a maximum hydrogen capacity of 4.0%. HUANG et al[11, 15] studied nanocrystallization and hydriding properties amorphous Mg₆₅Cu₂₅Nd₁₀ prepared by melt spinning. They reported that amorphous Mg65Cu25Nd10 showed faster initial hydrogenation rate and higher hydrogen capacity (3.2%) than those at partially and completely crystallized microstructural states. In the present study, the ribbons that were melt-spun at the highest solidification rate contain substantial amounts of amorphous phase and fine nano-size particles, as shown in Fig.5. Therefore, the present melt-spun ribbon is expected to have a large hydrogen storage capacity due to the increase of grain-boundary regions and amorphous regions.

4 Conclusions

- 1) The grain size of melt-spun ribbon was remarkably reduced by increasing the solidification rate. The microcrystalline, nanocrystalline and amorphous microstructures were obtained by applying the surface velocity of the graphite wheel of 3.1, 10.5 and 20.9 m/s, respectively.
- 2) In the melt-spun alloys, the Mg₁₂Mm phase was prone to form instead of Mg₁₇Mm₂ phase. The optimal microstructure with a considerable amount of nanocrystalline Mg and Mg₂Ni as well as amorphous phase is expected to have hydrogen storage properties. Mischmetal-containing phases of Mg₁₂Mm and Mg₁₇Mm₂ particles precipitated at the boundaries of Mg grains are expected to be beneficial for a rapid hydrogen diffusion path.

Acknowledgments

The authors are grateful to the Norwegian Research Council for financial support.

References

- SPASSOV T, KOSTER U. Thermal stability and hydriding properties of nanocrystalline melt-spun Mg₆₃Ni₃₀Y₇ alloy [J]. J Alloys Compd, 1998, 279: 279–286.
- [2] SPASSOV T, KOSTER U. Hydrogenation of amorphous and nanocrystalline Mg-based alloys [J]. J Alloys Compd, 1999, 287: 243–250.
- [3] SPASSOV T, LYUBENOVA L, KOSTER U, BARO M D. Mg-Ni-RE nanocrystalline alloys for hydrogen storage [J]. Mat Sci Eng A, 2004, 375–377: 794–799.
- [4] YAMAMURA S I, KIM H Y, KIMURA H, INOUE A, ARATA Y. Thermal stabilities and discharge capacities of melt-spun Mg-Ni-based amorphous alloys [J]. J Alloys Compd, 2002, 339: 230–235
- [5] ZALUSKA A, ZALUSKI L, STROM-OLSEN J O. Synergy of hydrogen sorption in ball-milled hydrides of Mg and Mg₂Ni [J]. J Alloys Compd, 1999, 289: 197–206.
- [6] ORIMO S, FUJII H, IKEDA K. Notable hydriding properties of a nanostructured composite material of the Mg₂Ni-H system synthesized by reactive mechanical grinding [J]. Acta Mater, 1997, 45: 331–341.
- [7] HONG S H, KWON S N, BAE J S, SONG M Y. Hydrogen-storage properties of gravity cast and melt spun Mg-Ni-Nb₂O₅ alloys [J]. Int J Hydrogen Energy, 2009, 34: 1944–1950.
- [8] KALINICHENKA S, RONTZSCH L, KIEBACK B. Structural and hydrogen storage properties of melt-spun Mg-Ni-Y alloys [J]. Int J Hydrogen Energy, 2009, 34: 7749–7755.
- [9] HUANG L J, TANG J G, WANG Y, LIU Ji-Xian, Wu D C. Effects of microstructure on the electrode properties of melt-spun Mg-based amorphous alloys [J]. J Alloys Compd, 2009, 485: 186–191.
- [10] SPASSOV T, RANGELOVA V, NEYKOV N. Nanocrystallization and hydrogen storage in rapidly solidified Mg-Ni-RE alloys [J]. J Alloys Compd, 2002, 334: 219–223.
- [11] HUANG L J, LIANG G Y, SUN Z B, ZHOU Y F. Nanocrystallization and hydriding properties of amorphous melt-spun Mg₆₃Cu₂₅Nd₁₀ alloy [J]. J Alloys Compd, 2007, 432: 172–176.
- [12] WU Y, HAN W, ZHOU S X, LOTOTSKY M V, SOLBERG J K, YARTYS V A. The effect of solidification rate on microstructural evolution of a melt-spun Mg-20Ni-8Mm hydrogen storage alloy [J]. J Alloys Compd, 2008, 446: 176–181.
- [13] WU Y, LOTOTSKY M V, SOLBERG J K, YARTYS V A, HAN W, ZHOU S X. Microstructure and novel hydrogen storage properties of melt-spun Mg-Ni-Mm alloys [J]. J Alloys Compd, 2009, 477: 262–266.
- [14] SPASSOV T, KOSTER U. Nanocrystalline Mg-Ni-based hydrogen storage alloys produced by nanocrystallization[J]. Mat Sci Forum, 1999, 307: 197–202.
- [15] HUANG L J, LIANG G Y, SUN Z B. Hydrogen-storage properties of amorphous Mg-Ni-Nd alloys [J]. J Alloys Compd, 2006, 421: 279–282

快淬 Mg-10Ni-2Mm 储氢合金的组织演化

武 英 1,2,3, 邢 娜 1,4, 卢志超 1, 韩 伟 1, 周少雄 1, J. K. SOLBERG2, V. A. YARTYS2,3

- 1. 中国钢研科技集团有限公司 安泰科技股份有限公司, 北京 100081;
 - 2. 挪威科技大学 材料技术系,特隆赫姆 7491,挪威;
 - 3. 挪威能源技术研究所, Kjeller N-2027, 挪威;
 - 4. 内蒙古工业大学 材料科学与工程学院, 呼和浩特 100051

摘 要: 研究一种镁基 Mg-10Ni-2Mm(摩尔分数,%)储氢合金在不同凝固速率下的组织演化。结果表明: 增加凝固速率可以大幅度细化合金条带的晶粒; 采用的石墨冷却轮表面速度为 3.1, 10.5 和 20.9 m/s 时,可以分别获得微晶、纳米晶和非晶组织; 当冷却轮盘表面速度为 3.1 m/s 时,快淬试样完全结晶化,组织中除了少量富 Mm 晶粒外,形成了粗大的 Mg 和 Mg₂Ni 微晶; 加快冷却轮盘表面速度到 10.5 m/s 时,大量的纳米颗粒形成,组织由大量的 Mg 和 Mg₂Ni 纳米晶组成; 进一步加快速度到 20.9 m/s 时,形成了包括非晶和纳米晶的混合组织。理想的组织是非晶基体上析出大量纳米晶,这样的组织有望获得最大的储氢容量和优异的吸放氢动力学。

关键词:储氢材料;镁基合金;快速凝固;组织;透射电镜

(Edited by YANG Hua)